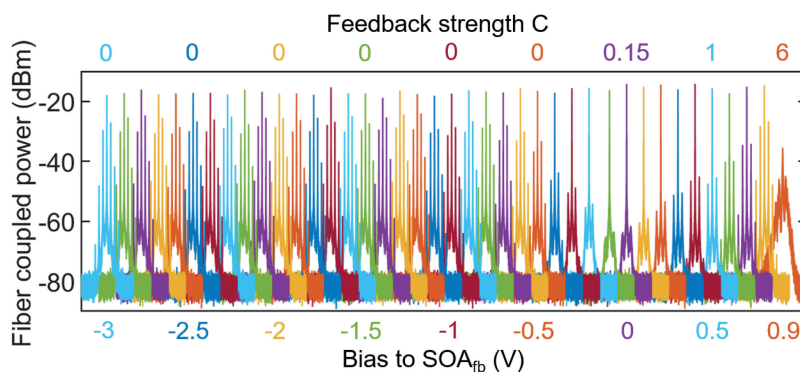


Monolithically Integrated Multiwavelength Laser With Optical Feedback: Damped Relaxation Oscillation Dynamics and Narrowed Linewidth


Volume 10, Number 6, December 2018

Dan Zhao, *Student Member, IEEE*
Stefanos Andreou, *Student Member, IEEE*
Weiming Yao, *Member, IEEE*
Daan Lenstra, *Senior Member, IEEE*
Kevin Williams, *Member, IEEE*
Xaveer Leijtens, *Senior Member, IEEE*



DOI: 10.1109/JPHOT.2018.2876382
1943-0655 © 2018 CCBY

Monolithically Integrated Multiwavelength Laser With Optical Feedback: Damped Relaxation Oscillation Dynamics and Narrowed Linewidth

Dan Zhao , *Student Member, IEEE*,
Stefanos Andreou, *Student Member, IEEE*,
Weiming Yao , *Member, IEEE*,
Daan Lenstra , *Senior Member, IEEE*,
Kevin Williams, *Member, IEEE*,
and Xaveer Leijtens , *Senior Member, IEEE*

Institute for Photonic Integration, Eindhoven University of Technology, Eindhoven 5612 AJ,
The Netherlands

DOI:10.1109/JPHOT.2018.2876382

1943-0655 © 2018 CCBY. This work is licensed under a Creative Commons Attribution 3.0 License.
For more information, see <http://creativecommons.org/licenses/by/3.0/>

Manuscript received July 18, 2018; revised October 7, 2018; accepted October 11, 2018. Date of publication October 16, 2018; date of current version October 30, 2018. This work was supported in part by the Netherlands Organization for Scientific Research domain Applied and Engineering Sciences, which was carried out under the Memphis Project 13538 and in part by the Dutch Technology Foundation Netherlands Organization for Scientific Research (NWO) for Project 13538. This paper was presented in part at the 44th European Conference on Optical Communication, Roma, Italy, September 23–27, 2018 [1]. Corresponding author: Dan Zhao (e-mail: d.zhao@tue.nl).

Abstract: An InP-based, monolithically integrated multiwavelength laser with optical feedback is presented. We demonstrate the performance of the dual-wavelength operation. Single-mode lasing is obtained for each of the two channels within a temperature range from 16 to 30 °C and an injection current range from 30 to 70 mA without mode-hopping. This is due to the combined filtering functions of an arrayed waveguide grating and a distributed Bragg reflector. A method that makes use of weak optical feedback is demonstrated to improve the stability of each single-mode. With this method, sustained relaxation oscillations that are excited by on-chip parasitic reflections are damped and linewidths in both channels are narrowed to around 400 kHz compared to the linewidth of 1 MHz that is obtained when no feedback is applied. The suppression ratio of the relaxation-oscillation-induced side peaks is measured to be over 45 dB for two simultaneously operated channels.

Index Terms: Semiconductor laser, arrayed waveguide grating, distributed Bragg reflector, single-mode, optical feedback, relaxation oscillation, linewidth.

1. Introduction

Monolithically integrated multi-wavelength lasers (MWLs) are key components for optical comb sources and wavelength-division multiplexing (WDM) systems [2]. Such MWLs require a high stability in order to support high-order modulation formats [3]. Lasers exhibit relaxation oscillations (ROs) which are caused by an intrinsic resonance between laser intensity and population inversion [4]. Sustained ROs in MWLs increase the relative intensity noise (RIN) around the RO-frequency and broaden the laser linewidth [5]. Therefore, they reduce the stability of MWLs

which limits their application domain. The occurrence of sustained ROs is sensitive to optical feedback and ROs can be enhanced or damped depending on the feedback properties including strength, phase and round-trip delay time [6]–[8]. In multi-wavelength lasers, the on-chip parasitic reflections which occur in many components such as arrayed waveguide gratings (AWGs) and multi-mode interference (MMI) couplers lead to weak optical feedback [9]. Sustained ROs were shown to be excited by weak optical feedback [5], and they are difficult to be damped if the weak feedback is induced by parasitic reflections as such reflections are random and uncontrollable. The occurrence of sustained ROs increases with device complexity.

By contrast, the integration of lasers with properly designed optical feedback show great potential on compression of ROs [7], [10]–[13] and improving modulation bandwidth [14], [15]. By fulfilling the RO-damped condition proposed in Ref. [7], lasers with weak feedback behave as lasers without feedback. The condition is that the product of the external round-trip delay time τ and the RO-frequency f_{RO} , which depends on the pump and threshold current of the lasers, equals a small integer, $\tau f_{RO} \cong 1, 2, 3, \dots$. Specifically, the time-dependent equations of a single-mode semiconductor lasers exposed to weak optical feedback obtained from the Lang-Kobayashi equations [7] can be reduced to a simpler set which is equivalent to the dynamical equations for a laser without feedback when the RO-damped condition is satisfied. This means that ROs are compressed for all feedback phase values when lasers are pumped into this RO-damped condition [7]. The prediction is valid in the regime of weak feedback, where the feedback coupling factor C that describes the feedback strength is smaller than 1. The unit-less factor C is given by [6]:

$$C = \gamma\tau\sqrt{1 + \alpha^2} \quad (1)$$

where α is the linewidth-enhancement parameter and γ is the feedback rate:

$$\gamma = \frac{r_{\text{ext}}(1 - r^2)}{\tau_{\text{in}}r} \quad (2)$$

where r_{ext} and r are the amplitude reflectivity of the external mirror and the laser mirror, respectively; τ_{in} is the internal round-trip time of the laser cavity. Parameters of a semiconductor laser with a feedback coupling factor $C \approx 0.3$ are given as an example: $\alpha = 2.6$, $\tau = 0.3$ ns, $r = 0.77$, $\tau_{\text{in}} = 15$ ps, $r_{\text{ext}} = 0.01$. The amplitude reflectivity of the external mirror r_{ext} corresponds to a 40 dB loss in the external feedback. The delay time τ should be a few tenths of nanoseconds for semiconductor lasers with an oscillation frequency f_{RO} of a few gigahertz. Pump current intervals exist that will fulfill the first few conditions [7]. Outside these intervals, the compression of ROs will be feedback-phase dependent. In that case, the laser is sensitive to phase fluctuations caused by temperature changes and off-chip ambient conditions.

Previously an experimental study was performed on a multi-wavelength laser with multi-mode interference reflectors (MIRs) with filtered optical feedback. It was not successful in fulfilling the RO-damped condition because the feedback round-trip delay time of hundredths of nanoseconds was too small. Therefore, it showed damped ROs with feedback-phase dependence [12]. A single-channel distributed Bragg reflector (DBR) based laser with feedback round-trip delay time of 0.3 ns has been demonstrated, showing damped ROs for all feedback phase values, which matches the theoretical prediction [13].

In this paper, we experimentally demonstrate the performance of a multi-wavelength DBR laser with an integrated delayed optical feedback, realized with an AWG acting as filter and multiplexer, a MIR and a waveguide spiral which introduces a round-trip delay time of around 0.3 ns for all channels. The goal is to validate the theoretical prediction from Ref. [7] in the presence of on-chip parasitic reflections and to explore the feasibility of implementing the theory to multi-channel operation using a common external feedback. In addition, we explore the laser linewidth enhancement when ROs are damped.

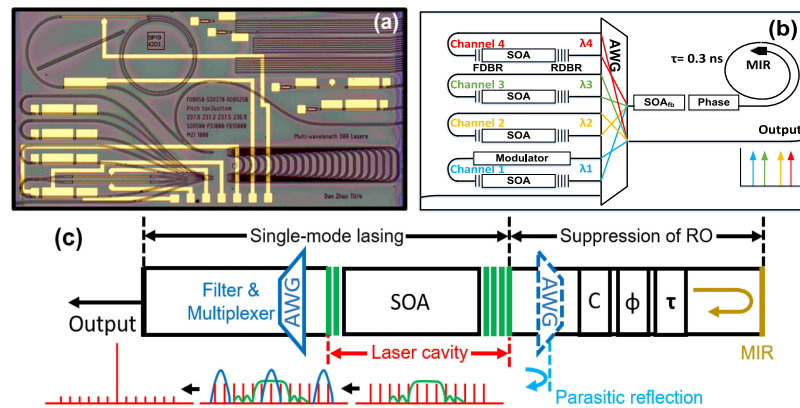


Fig. 1. (a) Microscope photograph and (b) schematic diagram of a monolithically integrated multi-wavelength DBR laser with delayed optical feedback. (c) An equivalent diagram of each looped channel if we unfold them.

2. Device Under Test

A microscope photograph and the schematic diagram of a monolithically integrated multi-wavelength DBR laser with delayed optical feedback are shown in Fig. 1(a) and (b), respectively. The devices were fabricated by Smart Photonics [16] through the JePPIX.eu multi-project wafer service [17]. The AWG has 9 inputs and 2 outputs with a channel spacing of 50 GHz and a free spectral range (FSR) of 450 GHz. The bottom left waveguide in Fig. 1(b) is used for characterizing the AWG. There are four DBR laser channels connected to the AWG inputs: adjacent inputs to the AWG connect to the two outputs of each DBR laser. In addition, there is a modulator in channel 1, which is included for evaluating its modulation performance for a future design of a multi-wavelength transmitter. However, it is not relevant with this work and will not be discussed further. The laser emission from the front-DBR (FDBR) is filtered and multiplexed through the AWG (solid lines). The Bragg wavelengths of the DBRs in the four channels are tuned to match the central wavelengths of the respective AWG passbands λ_1 , λ_2 , λ_3 , λ_4 , leading to the selection of a single-mode. The working principle is shown in the single-mode lasing section in Fig. 1(c), which is an equivalent diagram of each looped channel if we unfold them. The product of the filtering functions of the DBR (green line) and the AWG (blue line) selects only one longitudinal mode thus obtaining single-mode operation.

As shown in Fig. 1(b), the laser emission from the rear-DBR (RDBR) is filtered and multiplexed by the same AWG (dashed lines) and connected to a common MIR with a measured power reflectivity of 80% [18]. The upper inputs of the AWG towards the lower output (solid lines) have the same passbands as the lower inputs towards the upper output (dashed lines). In the external feedback cavity, there is a 500- μm -long SOA_{fb} and a 1000- μm -long phase shifter for controlling the feedback coupling factor C and feedback phase ϕ and a waveguide spiral to set an external round-trip delay time τ of 0.3 ns. The optical feedback coupling factor C can be controlled by the operating conditions of the SOA_{fb} to suppress the excited ROs of the single-mode lasers caused by the parasitic reflection from the AWG.

The DBR lasers have a grating pitch of 236.9, 237.5, 237.2 and 237.8 nm and are otherwise identical. They consist of a 370- μm -long SOA, a 50- μm -long front-DBR and a 250- μm -long rear-DBR with a designed coupling coefficient κ of 50 cm^{-1} . The passbands of the fabricated AWG may deviate from the design values with a maximum value of one FSR (450 GHz). Since the DBRs have a bandwidth of about 250 GHz and a blue tuning range of about 150 GHz, they cannot be aligned to AWG passbands when the offset between a DBR and a AWG passband is greater than 400 GHz. We have deliberately introduced wavelength offsets of $(50 + 450)$ GHz into two DBR lasers. The 50 GHz is to ensure sufficient alignment of at least two channels. The shift of one FSR was meant for separation of the two groups of channels which is not really necessary.

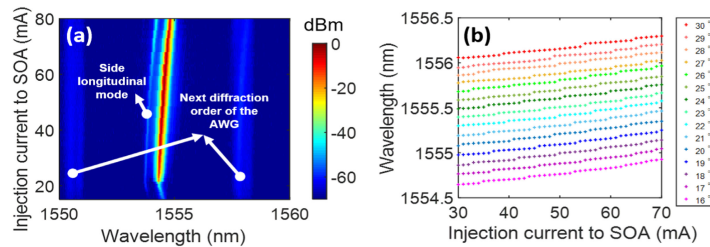


Fig. 2. (a) The optical spectra as a function of the injection current to the laser SOA in channel 2, measured with an optical spectrum analyzer with a resolution of 0.05 nm. The colour bar shows the output power in dBm. (b) Lasing wavelength position of the single-mode over a current range from 30 to 70 mA and a temperature range from 16 to 30 °C, measured with an optical spectrum analyzer with a resolution of 0.16 pm.

3. Single-Mode Lasing

The laser behavior of each channel is first studied when the feedback is switched off by applying a bias of -3 V to the SOA_{fb} . The laser SOA is pumped to provide gain and the rear-DBR is biased to align to one of the AWG passbands. The front-DBR is so short that its wavelength selection band is nearly flat in the operation range of the laser. A lensed anti-reflection coated fiber placed at the angled output of the laser is used to collect the light. An optical isolator (ISO) is connected to the fiber to prevent undesired back reflections into the laser.

The laser first operates at 18 °C set by a thermoelectric cooler (TEC). An optical spectrum analyzer (OSA) with a resolution of 0.05 nm (ANDO AQ-6315) is used to record the lasing spectra presented in Fig. 2(a). It shows the optical spectrum as a function of the injection current to the laser SOA in channel 2. The color bar shows the fiber coupled output power in dBm. The central mode at around 1554.5 nm is the lasing mode. One side longitudinal mode appears with 0.45 nm offset from the lasing mode and two additional modes appear further with an offset of 3.6 nm from the lasing mode created by the next diffraction order of the AWG. Single-mode operation is observed for an injection current range of 60 mA. We measured the lasing wavelength position over a current range from 30 to 70 mA and a temperature range from 16 to 30 °C. An OSA with a high resolution of 0.16 pm (APEX AP2041B) is used to obtain a better resolution of the lasing wavelength. Fig. 2(b) shows how the lasing wavelength shifts as the current or temperature increases. There is no mode-hopping to other longitudinal modes supported by the laser cavity, with a spacing of 0.45 nm. It indicates a high stability under changing external conditions. Due to the presence of parasitic reflection from the AWG, an extra, longer cavity is formed with that reflection and the DBR which results in longitudinal modes with a spacing of 0.05 nm. Mode-hops among those modes are visible in Fig. 2(b) and cannot be avoided.

4. Relaxation Oscillation Compression

A single channel of the laser is first pumped into the RO-damped condition, the spectra at different feedback coupling factor C are recorded with the high resolution OSA. As the feedback delay time is 0.3 ns, the RO-frequency should be 3.3 GHz to satisfy the first damped condition, where $\tau f_{RO} \cong 1$. The pump current for this laser is estimated according to the expected RO-frequency and known threshold current [7], [13], which is 36 ± 3 mA. The bias to the SOA_{fb} is adjusted from -3 to 0.9 V with a step of 0.1 V. There is no electrical input to the feedback phase shifter. The corresponding feedback coupling factor C is estimated according to Eq. (1) and (2). In our case, the amplitude reflectivity of the external mirror r_{ext} is determined by the insertion loss of the AWG, the propagation loss of the waveguide, the bias to the SOA_{fb} and the reflectivity of the MIR. The gain and absorption values of the SOA_{fb} used for calculating C are from Ref. [19], [20]. The feedback coupling factor C is in fact a function of the gain/absorption of the SOA_{fb} when adjusting the bias. The factor C increases from 0 to 6 (i.e. $r_{\text{ext}} \approx 0.21$ or a feedback loss of about 13.5 dB) by varying the bias to the SOA_{fb} from -3 to 0.9 V as shown in Fig. 3. The measured laser optical spectra are shown in Fig. 3 in order

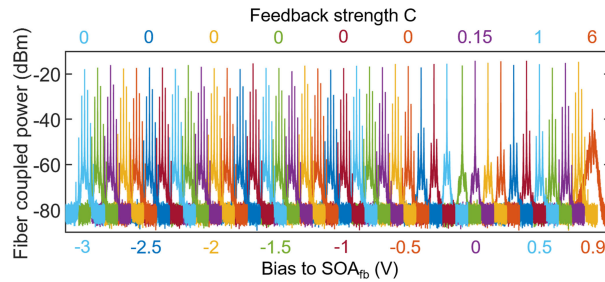


Fig. 3. Laser spectra of channel 2 for different values of the bias to the SOA_{fb} with corresponding feedback coupling factor C , when operated inside the stable current intervals ($I = 36$ mA).

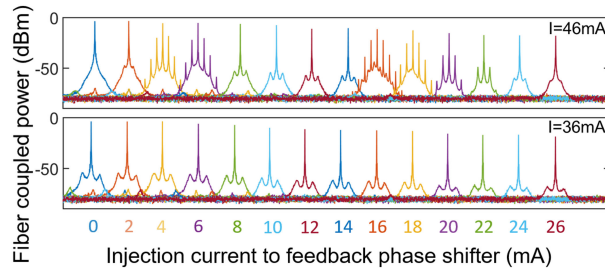


Fig. 4. Laser spectra of channel 2 for different values of the injection current I_{ϕ} to the feedback phase shifter, when operated outside the stable current intervals ($I = 46$ mA) and inside them ($I = 36$ mA).

of increasing values of the bias voltage of the SOA_{fb} , as indicated along the horizontal axis, where each spectrum has a wavelength span of 0.3 nm. The spectra show side peaks with amplitudes depending on the feedback coupling factor C . The obtained RO-frequency was verified according to the side-peak spacing and matches the expected value. When the feedback coupling factor C equals 0, the single-mode laser suffers from sustained ROs excited by the parasitic reflections. Other possible causes of ROs, such as thermal noise and spontaneous emission, are excluded by having a RO-damped isolated three-section DBR laser on the same chip. The ROs are damped and more than 30 dB suppression ratio (SR), the ratio between the lasing peak and the highest RO-induced peak, is obtained at bias values between -0.3 and 0.5 V. The corresponding feedback coupling factor C is between 0 and 1, which fits the theory well.

The bias to the SOA_{fb} is then set to 0.1 V, which is in the center of the damped region. The RO-sensitivity to the injection current I_{ϕ} to the feedback phase shifter is studied for two different pump currents of the laser. One pump current is inside the first stable interval that satisfies the RO-damped condition ($I = 36$ mA), the other is somewhere in the unstable region ($I = 46$ mA). The injection current I_{ϕ} to the phase shifter varies from 0 to 26 mA in 2 mA steps. This achieves over 2π phase modulation of the phase shifter, which was verified by tuning one arm of a test Mach-Zehnder modulator. Measured laser spectra for both cases are shown in Fig. 4. For the case with a pump current of 46 mA, it shows a RO-dependence on the feedback phase value, I_{ϕ} . Phase shifts more than 2π in the external delay are indeed obtained, as is evidenced by the periodic occurrence of ROs. For the case with a pump current of 36 mA, damped-ROs are observed over the full 2π feedback phase shift interval as predicted by the theory.

5. Linewidth Narrowing

A theoretical expression for the variation of the linewidth $\Delta\nu$ versus the external phase ϕ is given in Ref. [21] as:

$$\Delta\nu = \frac{\Delta\nu_0}{[1 + C \cos \phi]^2} \quad (3)$$

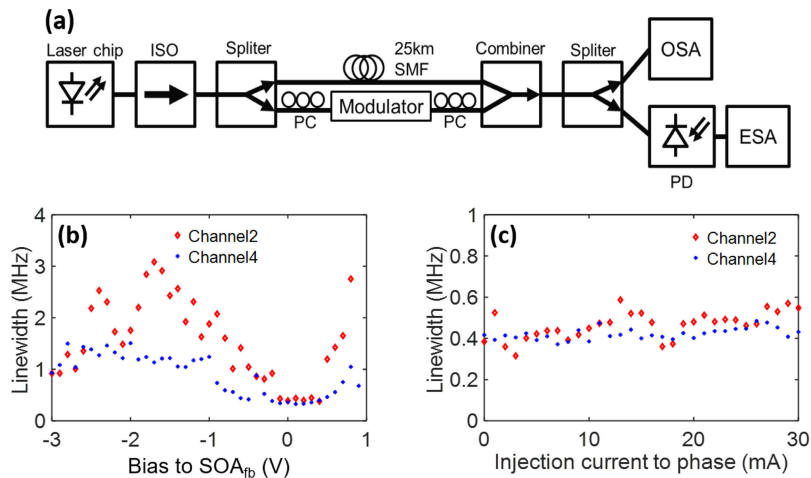


Fig. 5. (a) The schematic diagram of the linewidth characterization setup based on a delayed self-heterodyne method. PC is polarization controller; PD is photo detector; ESA is electrical spectrum analyser; The characterized FWHM linewidth as functions of (b) the bias to the SOA_{fb} and (c) the injection current I_{ϕ} to the feedback phase shifter when operating channel 2 and 4 independently. The pump currents for both channels are 36 mA which is within the first RO-damped stable current interval.

where $\Delta\nu_0$ is the intrinsic linewidth of the single-mode laser, which is considered as the averaged value at all injection currents I_{ϕ} to the phase shifter. The linewidth is measured with a setup based on a delayed self-heterodyne method [22] as shown in Fig. 5(a). A delay is introduced to one of the arms by using a 25 km single-mode fiber (SMF). The high resolution OSA is used for detecting the optical signals and an electrical spectrum analyzer (ESA) is used for detecting the electrical signals. The resolution and video bandwidth for electrical spectrum measurements are 30 kHz and 300 Hz, respectively. The laser is pumped with an injection current of 36 mA which was demonstrated to be within the first RO-damped stable current interval. Fig. 5(b) shows the FWHM linewidths as a function of the bias to the SOA_{fb} between -3 to 0.9 V with a step of 0.1 V when operating channel 2 and 4 independently. The minimum linewidths for both channel 2 and 4 are observed at bias to SOA_{fb} between -0.1 and 0.4 V, corresponding to the damped ROs. Then the bias to the SOA_{fb} is set to 0.1 V. The measured FWHM linewidths as a function of the injection current I_{ϕ} to the feedback phase shifter when operating channel 2 and 4 independently are shown in Fig. 5(c). The injection current I_{ϕ} to the feedback phase shifter is between 0 to 30 mA with a step of 1 mA, the current range corresponds to a feedback phase interval larger than 2π . The linewidth varies along with the injection current I_{ϕ} to the phase shifter within the ranges of 316 to 587 kHz and 371 to 484 kHz for channel 2 and 4, respectively. According to eq. (3), the linewidth is very sensitive to phase when C is close to 1 while it is nearly constant when C is close to 0. The feedback coupling factors C are calculated to be 0.15 and 0.07 for channel 2 and 4 respectively according to Eq. 3, which match well with our estimation.

6. Multi-Channel Performance

Lasing spectra of the laser when operating the four channels independently with different bias to the SOA_{fb} and when operating them simultaneously with a bias of 0.1 V applied to the common feedback are shown in Fig. 6(a) and (b), respectively. The fiber coupled output power in each channel is determined by the emitted power from the front-DBR, the AWG insertion loss, the agreement between the AWG passband and the DBR stopband, the waveguide propagation loss and the fiber-to-waveguide coupling loss. The fiber coupled power from the front-DBR of a stand-alone three-section DBR laser is measured to be about 5 dB at an injection current of 36 mA. The sum of the AWG insertion loss and the waveguide propagation loss are slightly more than 5 dB. If

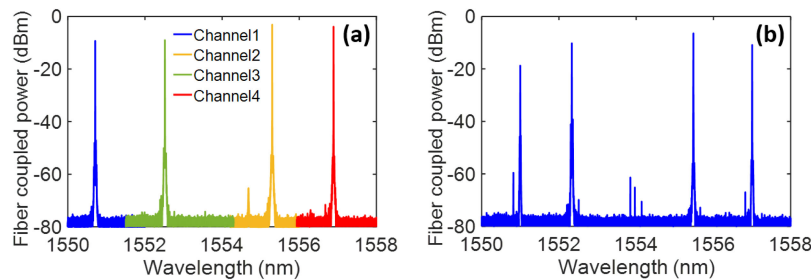


Fig. 6. Lasing spectra of the laser while operating four channels (a) independently and (b) simultaneously.

the agreement between the AWG passband and the DBR stopband is poor, there will be an extra loss. All above lead to a final output power of around 0 dBm or less. They show less compressed ROs in channel 1 and 3 compared to channel 2 and 4, indicated by the smaller SRs. This is due to the pump currents for channel 1 and 3, that are inside the unstable current intervals while for channel 2 and 4 they are inside the stable current intervals. The problem for channel 1 and 3 is that the wavelength mismatches between the AWG passbands and the DBRs are slightly beyond the tuning range of the DBR. The lasing conditions can be fulfilled by not only tuning the DBR but also pump the laser with a high current and sometimes with the help of a strong feedback. The large wavelength offsets were deliberately introduced in the design in order to guarantee at least two working channels. Fig. 6(a) shows a SR of above 38 dB for channel 1 and 3 and of above 50 dB for channel 2 and 4. Fig. 6(b) shows a SR of above 26 dB for channel 1 and 3 and of above 45 dB for channel 2 and 4. With improved fabrication precision, the AWG passbands and the DBR stopbands can be matched which will enable true multi-channel operation with more than 45 dB SR.

7. Conclusion

We experimentally demonstrate an InP-based, monolithically integrated multi-wavelength DBR laser with weak optical feedback which has a broad single-mode lasing range in each channel and is insensitive to the parasitic reflections at RO-damped conditions. This is demonstrated by the reduced relaxation oscillation dynamics and by the narrowed laser linewidth. The linewidth is almost insensitive to the feedback phase and was maintained to around 400 kHz which shows a good stability of the laser.

References

- [1] D. Zhao, S. Andreou, W. Yao, K. Williams, and X. Leijtens, "Monolithically integrated multi-wavelength DBR laser with damped relaxation oscillation dynamics," in *Proc. 44th Eur. Conf. Opt. Commun.* Rome, Italy, 2018, Paper Tu1C.3.
- [2] R. Piramidowicz, S. Stopinski, K. Lawniczuk, P. Szczepanski, X. Leijtens, and M. Smit, "Photonic integrated circuits a new approach to laser technology," *Bull. Polish Acad. Sci., Tech. Sci.*, vol. 60, no. 4, pp. 683–689, 2013.
- [3] M. Seimetz, "Laser linewidth limitations for optical systems with high-order modulation employing feed forward digital carrier phase estimation," in *Proc. Opt. Fiber Commun. Conf./Nat. Fiber Opt. Eng. Conf.*, 2008, Paper OTuM2. [Online]. Available: <http://www.osapublishing.org/abstract.cfm?URI=OFC-2008-OTuM2>
- [4] K. Petermann, *Laser Diode Modulation and Noise*. Kluwer Academic Publishers P.O. Box 17,3300 AA Dordrecht, The Netherlands: in co-publication with KTK Scientific Publishers (KTK), Tokyo, Japan, 1988.
- [5] C. Masoller and N. B. Abraham, "Stability and modulation properties of a semiconductor laser with weak optical feedback from a distant reflector," *Quantum Semiclassical Opt., J. Eur. Opt. Soc. Part B*, vol. 10, no. 3, pp. 519–534, 1998. [Online]. Available: <http://stacks.iop.org/1355-5111/10/i=3/a=010>
- [6] G. Acket, D. Lenstra, A. D. Boef, and B. Verbeek, "The influence of feedback intensity on longitudinal mode properties and optical noise in index-guided semiconductor lasers," *IEEE J. Quantum Electron.*, vol. QE-20, no. 10, pp. 1163–1169, Oct. 1984.
- [7] D. Lenstra, "Relaxation oscillation dynamics in semiconductor diode lasers with optical feedback," *IEEE Photon. Technol. Lett.*, vol. 25, no. 6, pp. 591–593, Mar. 2013.

- [8] A. Uchida, *Optical Communication With Chaotic Lasers: Applications of Nonlinear Dynamics and Synchronization*. Hoboken, NJ, USA: Wiley, Jan. 2012.
- [9] E. Kleijn, M. Smit, and X. Leijtens, "Analysis of parasitic effects in PICs using circuit simulation," *Proc. SPIE*, vol. 8781, 2013, Art. no. 878104.
- [10] R. W. Tkach and A. R. Chraplyvy, "Regimes of feedback effects in 1.5- μm distributed feedback lasers," *J. Lightw. Technol.*, vol. 4, no. 11, pp. 1655–1661, Nov. 1986.
- [11] S. Donati and R. H. Horng, "The diagram of feedback regimes revisited," *IEEE J. Sel. Topics Quantum Electron.*, vol. 19, no. 4, Jul. 2013, Art. no. 1 500309.
- [12] J. Zhao, D. Lenstra, R. Santos, M. Wale, M. Smit, and X. Leijtens, "Stability of a monolithic integrated filtered-feedback laser," *Opt. Exp.*, vol. 20, no. 26, pp. B270–B278, Sep. 2012.
- [13] D. D'Agostino, H. P. M. M. Ambrosius, M. K. Smit, and D. Lenstra, "Integrated laser with optical feedback shows suppressed relaxation-oscillation dynamics," *IEEE Photon. Technol. Lett.*, vol. 27, no. 21, pp. 2292–2295, Nov. 2015.
- [14] M. Radziunas *et al.*, "Improving the modulation bandwidth in semiconductor lasers by passive feedback," *IEEE J. Sel. Topics Quantum Electron.*, vol. 13, no. 1, pp. 136–142, Jan. 2007.
- [15] G. Morthier, R. Schatz, and O. Kjebon, "Extended modulation bandwidth of DBR and external cavity lasers by utilizing a cavity resonance for equalization," *IEEE J. Quantum Electron.*, vol. 36, no. 12, pp. 1468–1475, Dec. 2000.
- [16] Mar. 2012. [Online]. Available: <http://www.smartphotonics.nl/>
- [17] X. Leijtens, "JePPIX: The platform for InP-based photonics," *IET Optoelectron.*, vol. 5, no. 5, pp. 202–206, 2011.
- [18] E. Kleijn, M. Smit, and X. Leijtens, "Multimode interference reflectors: A new class of components for photonic integrated circuits," vol. 31, no. 18, pp. 3055–3063, Sep. 2013.
- [19] D. Pustakhod, K. Williams, and X. Leijtens, "Fast and robust method for measuring semiconductor optical amplifier gain," *IEEE J. Sel. Topics Quantum Electron.*, vol. 24, no. 1, pp. 1–9, Jan. 2018.
- [20] D. Pustakhod, K. Williams, and X. Leijtens, "Method for polarization-resolved measurement of electroabsorption," *IEEE Photon. J.*, vol. 10, no. 2, Apr. 2018, Art. no. 6600611.
- [21] G. Agrawal, "Line narrowing in a single-mode injection laser due to external optical feedback," *IEEE J. Quantum Electron.*, vol. QE-20, no. 5, pp. 468–471, May 1984.
- [22] T. Okoshi, K. Kikuchi, and A. Nakayama, "Novel method for high resolution measurement of laser output spectrum," *Electron. Lett.*, vol. 16, no. 16, pp. 630–631, Jul. 1980.